Electronic Supplementary Material (ESI) for Soft Matter.

Electronic Supporting Information

Probing sedimentation non-ideality of particulate systems using analytical centrifugation

M. J. Uttinger[a,b], D. Jung[c], N. Dao[a], H. Canziani[a,b], C. Lübbert[a,b], N. Vogel[a,b], W. Peukert[a,b], J. Harting[c,d], J. Walter[a,b]

[a] Institute of Particle Technology (LFG), Friedrich-Alexander-Universität Erlangen-Nürnberg (FAU), Cauerstraße 4, 91058 Erlangen, Germany.

[b] Interdisciplinary Center for Functional Particle Systems (FPS), Friedrich-Alexander-Universität Erlangen-Nürnberg (FAU), Haberstraße 9a, 91058 Erlangen, Germany.

[c] Forschungszentrum Jülich, Helmholtz Institute Erlangen-Nürnberg for Renewable Energy (IEK-11), Fürther Straße 248, 90429 Nürnberg, Germany.

[d] Department of Chemical and Biological Engineering and Department of Physics, Friedrich-Alexander-Universität Erlangen-Nürnberg, Fürther Straße 248, 90429 Nürnberg, Germany.

E-mail: johannes.walter@fau.de

Concentration dependence of the sedimentation coefficient

Figure S1 depicts a representative plot of the concentration-dependent inverse sedimentation coefficient. The apparent slope accounts for the concentration dependence of the sedimentation coefficient and can be related to the sedimentation coefficient extrapolated to infinite dilution to calculate k_s or K_s.

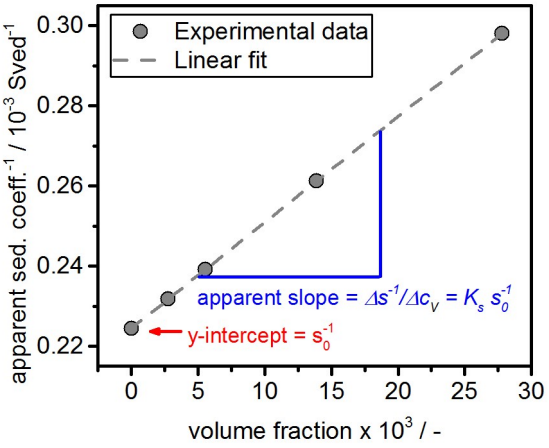

Figure S1: Schematic illustration depicting how to extract the apparent slope for the description of the concentration dependency and intercept at the ordinate for the extraction of the sedimentation coefficient at infinite dilution via AC.

Hindrance function

Given the case that the sedimentation velocity gradually decreases with the volume fraction, the sedimentation coefficient can be obtained when introducing the hindrance function h_{hind} according to:[1,2]

$$s = \frac{(\rho_P - \rho_F) \cdot x^2}{18\eta} \cdot h_{hind}(c_V) \tag{S1}$$

h_{hind} is expressed as a function of the particles' volume fraction c_V and the relative apparent viscosity η_{rel}:[1]

$$h_{hind}(c_V) = \frac{(1 - c_V)^2}{\eta_{rel}(c_V)} \qquad with \quad \eta_{rel}(c_V) = (1 - c_V)^{-n} \tag{S2}$$

The exponent n is a rheological coefficient, which depends on hydrodynamic non-ideality effects such as hindered settling and particle interactions.[1] Combination of Equations (S1) and (S2) and subsequent linearization leads to an expression of the sedimentation coefficient as a function of the volume fraction, which is equivalent to the relation given in Equation (5) in the main manuscript. From this expression, we can conclude that the description of the concentration dependence of the sedimentation properties through the Gralen coefficient and the hindrance function are equivalent and can thus be easily interchanged.

The hindrance function describes the dependency of the sedimentation velocity as a function of the volume fraction and rheological coefficient n according to:

$$\log(s) = (2 + n) \cdot \log(1 - c_V) + \log\left[\frac{(\rho_P - \rho_F) \cdot x^2}{18\eta}\right] \tag{S3}$$

Particle size distributions for silica and polystyrene particles

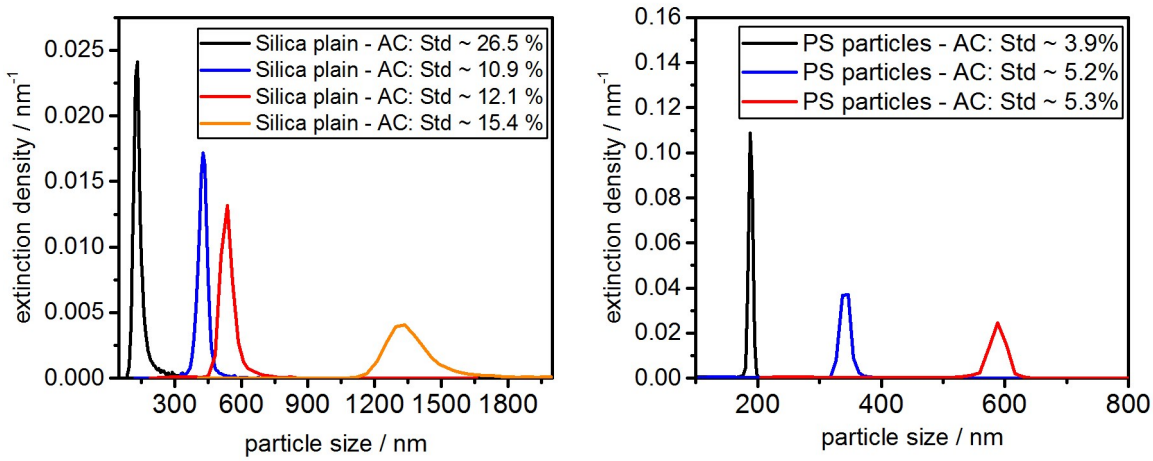

Figure S2: (Left) Particle size distributions of plain silica particles for different nominal particles sizes as measured by AC at low concentrations. The relative standard deviations of the particle size distributions are indicated in the legend. (Right) Particle size distributions for polystyrene (PS) particles for different nominal particles sizes as measured by AC at low concentrations. The relative standard deviations of the particle size distributions are indicated in the legend.

Conductivity measurements

For each sample, the conductivity was measured at various particle volume fractions. The data are shown in Figure S3 For each sample, a linear relationship between conductivity and the particle volume fraction was observed, which confirms the presence of a weak electrolyte.

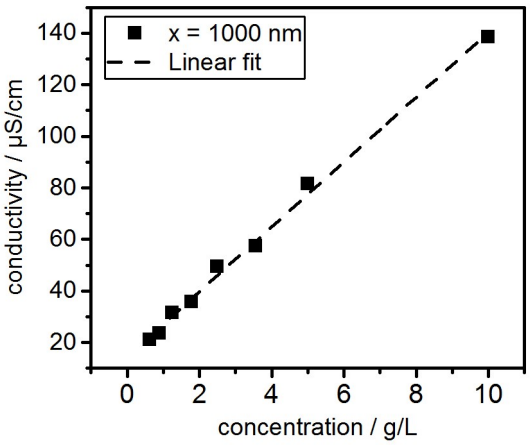

Figure S3: Measured conductivity of a particle dispersion at different particle concentrations. The nominal diameter of the silica particles in the dispersion was 1000 nm.

$$\Lambda_m = \frac{\mu}{c_m} \tag{S4}$$

Λ_m is the molar conductivity, μ is the conductivity and c_m is the ion concentration.

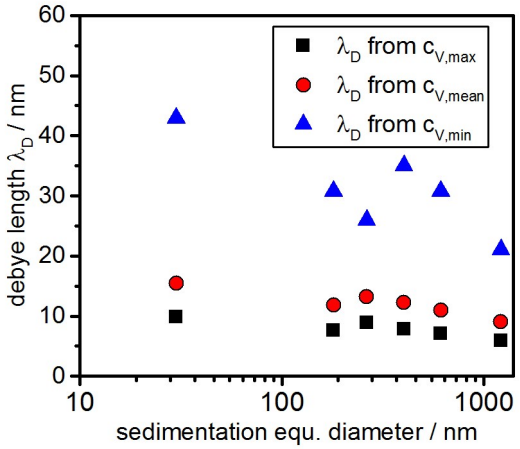

Figure S4: Experimentally determined Debye screening lengths of particle dispersions for various particle sizes for plain silica particles. The conductivity measurements were performed at various particle concentrations. The maximum, mean and minimum particle volume fractions were 0.0138, 5.5×10^{-3} and 5.5×10^{-4}, respectively, hence, covering the whole range of concentrations, which have been investigated within this study.

Lattice Boltzmann simulations

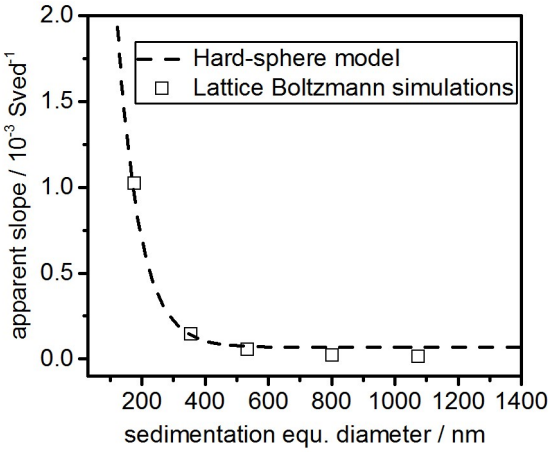

Figure S5: Apparent slope versus sedimentation equivalent diameter as retrieved from lattice Boltzmann simulations. The retrieved values are compared to the hard-sphere model, which is provided by a constant Gralen coefficient of K_s = 6.55.

Repulsion range

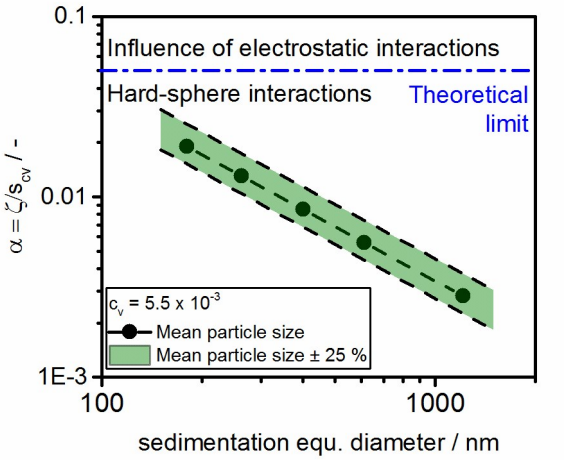

Figure S6: Repulsion range versus sedimentation equivalent diameter for silica particles with nominal sizes larger than 100 nm. The effect of polydispersity, which is taken into account as a change in particle size by 25 %, is indicated.

Effect of self-sharpening

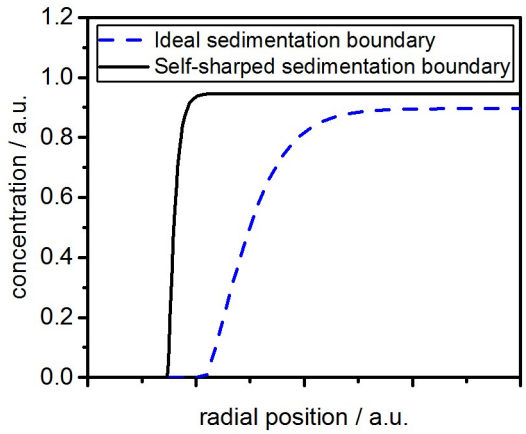

Figure S7: Exemplary sedimentation profile as observed in an SV-AC experiment for an ideal case (blue dashed line) and for the case of a strong concentration dependency of the sedimentation behavior (black line)

Normalized sedimentation velocity versus particle volume concentration

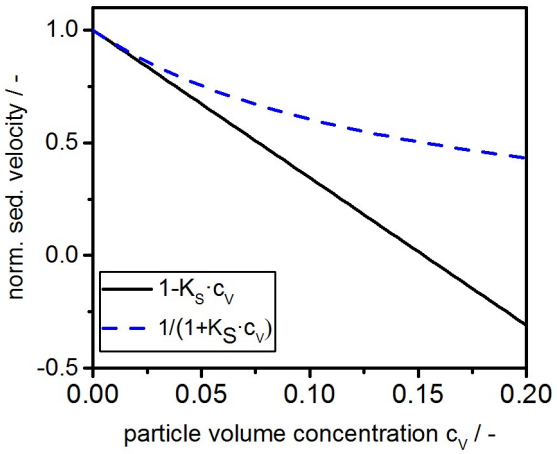

Figure S8: Normalized sedimentation velocity as calculated from Equation (7) (blue dashed line) and Equation (8) (black straight line) from the main manuscript as a function of the particle volume fraction.

Stability – Zeta potential

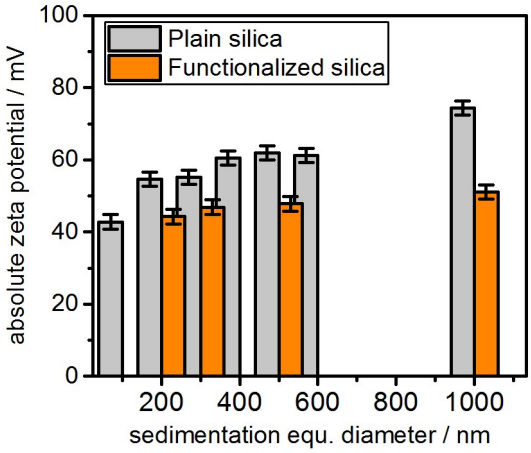

Figure S9: Zeta potentials for plain silica particles (grey bars) and surface-functionalized silica particles (orange bars) over a broad size range from 100 nm to 1000 nm.

Reproducibility of analytical centrifugation measurements

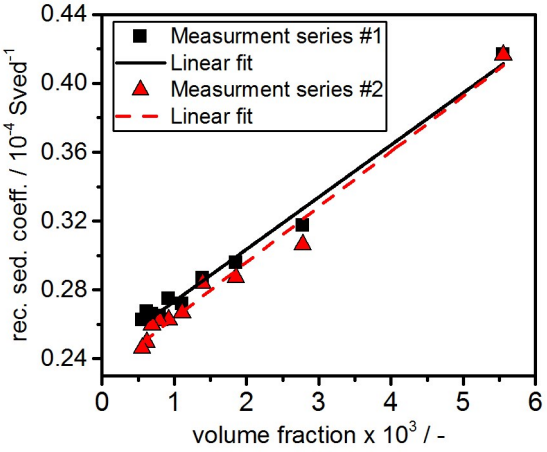

Figure S10: Reciprocal sedimentation coefficient as a function of particle concentration measured in two different AC experiments. Data points are indicated with circles, a linear fit was introduced as indicated by the lines. A perfect match of the two linear fits can be observed.

Measurement of Gralen coefficients for silica particles and error propagation for the Gralen coefficient and the apparent slope

The Gralen coefficient is denoted as k_s and describes the dependency of the sedimentation coefficient on the particle mass concentration. According to Equation (7) in the main manuscript, the parameter K_s describes the dependency of the sedimentation coefficient on the particle volume fraction. These two parameters can be used interchangeably.

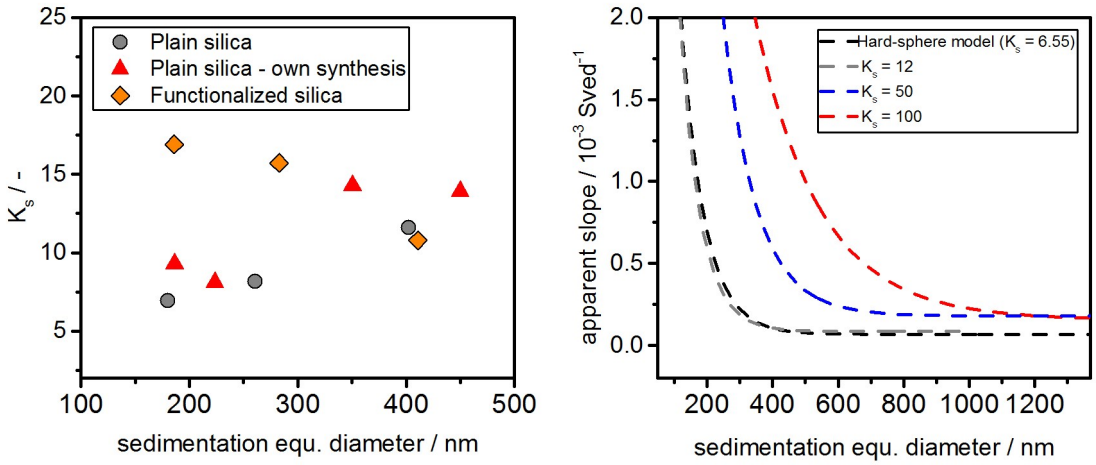

Figure S11: (Left) Gralen coefficients for plain silica particles with different sedimentation equivalent diameters. (Right) Theoretical apparent slope as a function of sedimentation equivalent diameter for different preset values of K_s.

In the following Equations ((S5) to (S10)) the error propagation of the Gralen coefficient k_s is calculated:

$$k_s = \frac{s_2 - s_1}{s_1 c_1 - s_2 c_2} \tag{S5}$$

$$\frac{\partial k_s}{\partial s_1} = \frac{s_2(c_2 - c_1)}{(s_1 c_1 - s_2 c_2)^2} \tag{S6}$$

$$\frac{\partial k_s}{\partial s_2} = \frac{s_1(c_2 - c_1)}{(s_1 c_1 - s_2 c_2)^2} \tag{S7}$$

$$\frac{\partial k_s}{\partial c_1} = -\frac{s_1(s_2 - s_1)}{(s_1 c_1 - s_2 c_2)^2} \tag{S8}$$

$$\frac{\partial k_s}{\partial c_2} = \frac{s_2(s_2 - s_1)}{(s_1 c_1 - s_2 c_2)^2} \tag{S9}$$

$$\Delta k_s = \sqrt{\left(\frac{\partial k_s}{\partial s_1} \cdot \Delta s_1\right)^2 + \left(\frac{\partial k_s}{\partial s_2} \cdot \Delta s_2\right)^2 + \left(\frac{\partial k_s}{\partial c_1} \cdot \Delta c_1\right)^2 + \left(\frac{\partial k_s}{\partial c_2} \cdot \Delta c_2\right)^2} \quad \text{(S10)}$$

Assuming a particle with a mean particle size of 200 nm, a sedimentation coefficient of 17822 Sved results. The sedimentation coefficients at c_1 = 0.1 g/L and c_2 = 12 g/L are s_1 = 17810 Sved and s_2 = 16524 Sved. We assume a maximum error for the concentration of 2 % and for the sedimentation coefficient of 1 %. Taking into account hard-sphere interactions, the value for K_s is 6.55. Considering Equation S9 and the parameters mentioned above, the error for the K_s value is calculated to be ± 0.8.

In the following Equations ((S11) to (S16)), the error propagation of the apparent slope is calculated:

$$X = \frac{\frac{1}{s_1} - \frac{1}{s_2}}{c_1 - c_2} \quad \text{(S11)}$$

$$\frac{\partial X}{\partial s_1} = \frac{-\frac{1}{s_1^2}}{c_1 - c_2} \quad \text{(S12)}$$

$$\frac{\partial X}{\partial s_2} = \frac{\frac{1}{s_2^2}}{c_1 - c_2} \quad \text{(S13)}$$

$$\frac{\partial X}{\partial c_1} = -\frac{\left(\frac{1}{s_1} - \frac{1}{s_2}\right)}{(c_1 - c_2)^2} \quad \text{(S14)}$$

$$\frac{\partial X}{\partial c_2} = \frac{\left(\frac{1}{s_1} - \frac{1}{s_2}\right)}{(c_1 - c_2)^2} \quad \text{(S15)}$$

$$\Delta X = \sqrt{\left(\frac{\partial X}{\partial s_1} \cdot \Delta s_1\right)^2 + \left(\frac{\partial X}{\partial s_2} \cdot \Delta s_2\right)^2 + \left(\frac{\partial X}{\partial c_1} \cdot \Delta c_1\right)^2 + \left(\frac{\partial X}{\partial c_2} \cdot \Delta c_2\right)^2} \quad \text{(S16)}$$

For the values given above, the error in the slope amounts to (6.62 ± 0.77)*10^{-4} $Sved^{-1}$.

Apparent slopes for plain silica particles dispersed in acetate buffer solutions

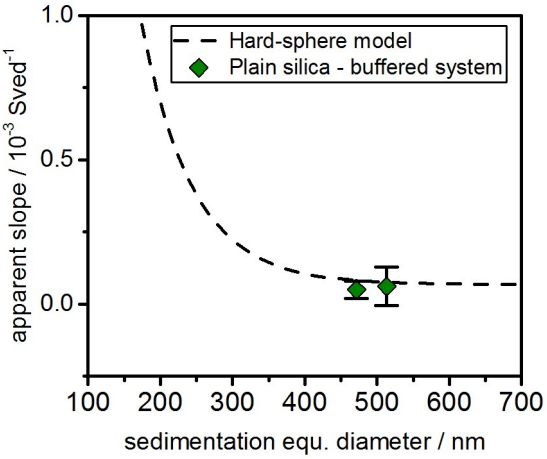

Figure S12: Apparent slope versus sedimentation equivalent diameter for plain silica particles. The experimental values for silica particles dispersed in a buffer solution are shown for comparison.

Particle interactions for polystyrene particles

Based on the results for silica particles, we tested the applicability of our method by transferring it to another material system, namely polystyrene particles. Notably, the polydispersity of the polystyrene particles is reduced with respect to the polydispersity of the silica particles (see both panels of Figure S2). However, polystyrene particles can be synthesized with a high surface charge[3], hence we believe the transfer of our protocol to this material system particles serves as a proof of principle for our protocol. Moreover, the sedimentation analysis of polystyrene particles via SV-AC is more challenging as the difference of the polystyrene particle density and the solvent density is much smaller.

We determined apparent slopes from AC experiments for various sedimentation equivalent diameters following the procedure for the silica particles. One representative result for polystyrene particles with a nominal diameter of 200 nm is presented in Figure S13 left, confirming a linear dependency of the reciprocal sedimentation coefficient as a function of the particle volume fraction. The measured apparent slopes versus the sedimentation equivalent diameter are depicted in Figure S13 right. The error bars indicate the uncertainties of the linear regressions.

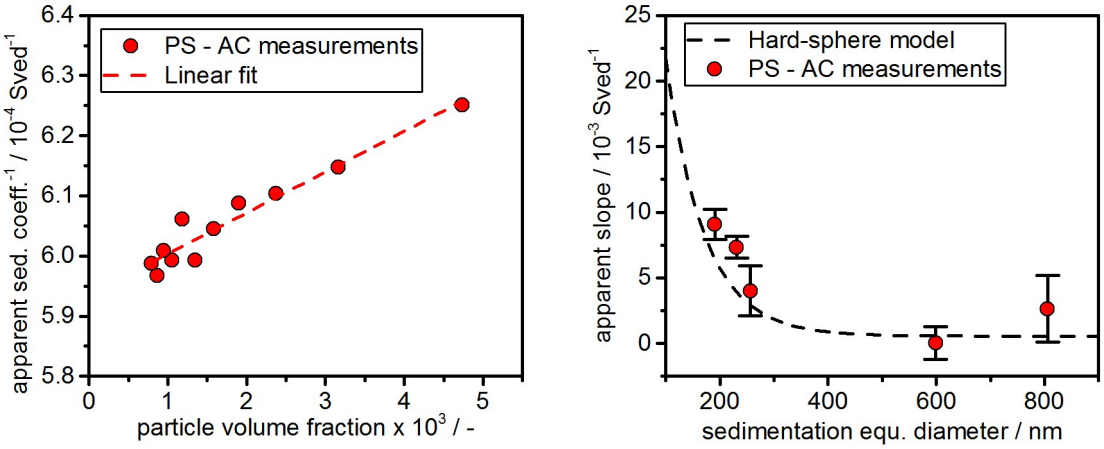

Figure S13: (Left) Reciprocal sedimentation coefficient versus volume fraction for polystyrene (PS) particles with a nominal diameter of 200 nm. The sedimentation coefficient at infinite dilution is obtained from extrapolation to zero concentration. The apparent slope is retrieved from a linear fit of the data. (Right) Apparent slope as a function of the sedimentation equivalent diameters for polystyrene particles (red circles). The hard-sphere model is indicated (black dashed line).

We further calculated the apparent slopes for polystyrene particles, assuming a hard-sphere model, which are presented alongside the measurement results in Figure S13 right. Slight deviations are attributed to the low density difference of polystyrene particles and water, which leads to minor instabilities due to small temperature fluctuations within the measured sedimentation boundaries.[4,5] It is evident that the sedimentation properties of polystyrene particles are governed by hard-sphere type particle interactions for sedimentation equivalent diameters spanning over a broad range of particle sizes. Our observations are in line with our expectations from theoretical considerations since the interparticle distances at a volume fraction of 0.01 are 560 nm, 1681 nm and 2242 nm for 200 nm, 600 nm and 800 nm sized polystyrene

particles, respectively. The two latter are even beyond the theoretical Debye length of pure water at pH 7, which is 953 nm at 20 °C. Notably, the Debye screening length of pure water is calculated based on the ion concentrations of OH^- and H^+, respectively. The respective repulsion ranges are therefore 1.78 x 10^{-2}, 5.93 x 10^{-3} and 4.45 x 10^{-3} when assuming a Debye screening length of 10 nm.

Therefore and as confirmed experimentally, electrostatic interactions of the investigated polystyrene particles are not expected to have a measurable effect on sedimentation non-ideality. Conclusively, our protocol for the investigation of interparticle interactions via sedimentation analysis has been successfully transferred from polydisperse silica particles to another material system with reduced polydispersity, which confirms our expectations and further underlies the applicability of our experimental approach.

Effect of polydispersity on the retrieved Gralen coefficient

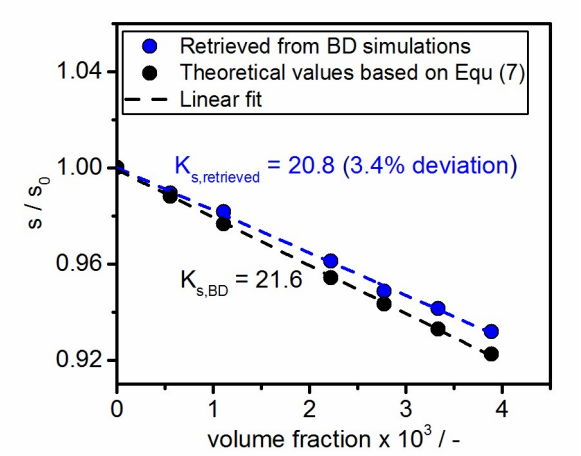

Figure S14: Apparent median sedimentation coefficients *s* normalized by the sedimentation coefficient at infinite dilution s_0 as retrieved from BD simulations (blue data points and dashed line) and normalized apparent sedimentation coefficients from Equation 7 (black data points and straight line).

Effect of self-sharpening from BD simulations

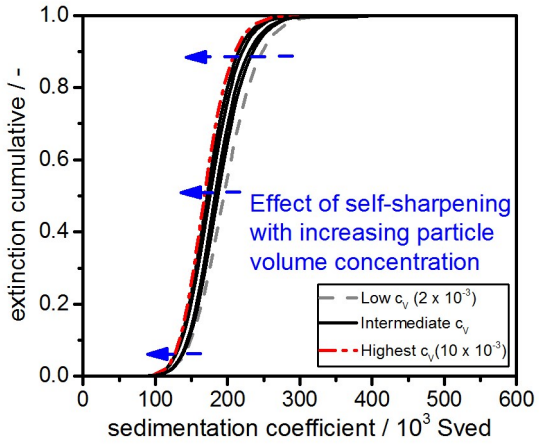

Figure S15: Cumulative sedimentation coefficient distributions at various particle volume fractions as retrieved from data analysis after hydrodynamic simulation. Data was simulated via BD simulations for silica particles with a mean particle size of 600 nm and a polydispersity of 10 %. Hydrodynamic non-ideality was included by considering a K_s value of 7.

Normalized measured sedimentation coefficient to the value at infinite dilution for 30 nm silica particles

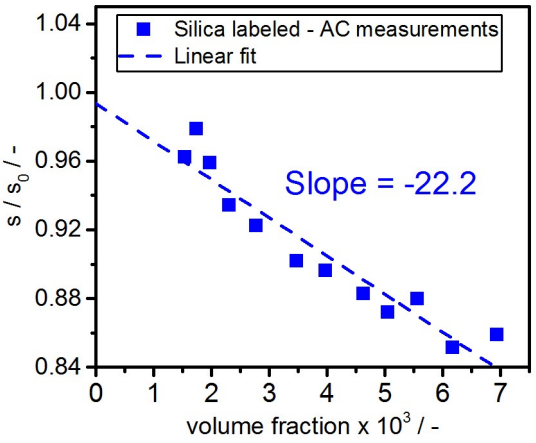

Figure S16: Measured normalized apparent sedimentation coefficients for fluorescent silica particles with a nominal diameter of 30 nm at various particle volume fractions. A linear fit was applied to the data for the determination of the slope.

References

(1) Antonopoulou, E.; Rohmann-Shaw, C. F.; Sykes, T. C.; Cayre, O. J.; Hunter, T. N.; Jimack, P. K. Numerical and experimental analysis of the sedimentation of spherical colloidal suspensions under centrifugal force. *Physics of Fluids* **2018**, *30* (3), 30702. DOI: 10.1063/1.5010735.

(2) He, P.; Mejia, A. F.; Cheng, Z.; Sun, D.; Sue, H.-J.; Dinair, D. S.; Marquez, M. Hindrance function for sedimentation and creaming of colloidal disks. *Physical review. E, Statistical, nonlinear, and soft matter physics* **2010**, *81* (2 Pt 2), 26310. DOI: 10.1103/PhysRevE.81.026310.

(3) Reese; Guerrero; Weissman; Lee; Asher. Synthesis of Highly Charged, Monodisperse Polystyrene Colloidal Particles for the Fabrication of Photonic Crystals. *Journal of colloid and interface science* **2000**, *232* (1), 76–80. DOI: 10.1006/jcis.2000.7190.

(4) Butenko, A. V.; Nanikashvili, P. M.; Zitoun, D.; Sloutskin, E. Critical onset of layering in sedimenting suspensions of nanoparticles. *Phys. Rev. Lett.* **2014**, *112* (18), 188301. DOI: 10.1103/PhysRevLett.112.188301.

(5) Nanikashvili, P. M.; Kapilov-Buchman, Y.; Israel, L. L.; Lellouche, J.-P.; Zitoun, D.; Butenko, A. V.; Sloutskin, E. Layering in sedimenting nanoparticle suspensions: The order-inducing role of randomness. *Colloids and Surfaces A: Physicochemical and Engineering Aspects* **2015**, *483*, 248–256. DOI: 10.1016/j.colsurfa.2015.04.005.